XI International Conference on Computational Methods for Coupled Problems in Science and Engineering
COUPLED PROBLEMS 2025
A. Larese, S. Perotto and G. Rozza (Eds)

NUMERICAL COUPLING OF A FVM AND FEM CODES APPLIED TO A LOW-PRANDTL TURBULENT SQUARE CAVITY

S. BALDINI[1], G. BARBI[1], A. CERVONE[1], F. GIANGOLINI[1,*], S. MANSERVISI[1] AND L. SIROTTI[1]

[1]Deparment of Industrial Engineering (DIN)
Alma Mater Studiorum - Università di Bologna
Lab. of Montecuccolini, 40136 Bologna, Italy
e-mail: federico.giangolini2@unibo.it

Key words: Coupled Problems, Low-Prandtl number fluids, Natural Convection, FEM, FVM

Abstract. This study investigates low-Prandtl-number fluids natural convection in a square differentially heated cavity, a canonical problem with relevance to liquid metal applications. Due to their technological importance, accurate prediction of flow and heat transfer in such regimes is essential. Two numerical strategies are assessed: standalone simulations with a finite element code (FEMuS) and with a finite volume code (OpenFOAM), and a coupled approach in which the two solvers are volumetrically linked via MEDCoupling. Results are benchmarked against reference DNS data.

1 INTRODUCTION

Heat transfer in liquid metals plays a crucial role in many engineering applications, such as high-performance cooling systems for next-generation nuclear reactors and solar energy collectors. In these contexts, natural convection often governs the heat transfer process. For instance, during the shutdown of a liquid metal nuclear reactor, heat removal from the core to the coolant occurs predominantly via natural convection, driven by the temperature gradient between the two.

Despite its importance, natural convection in liquid metals remains relatively poorly understood, particularly in confined enclosures where buoyancy-driven flows can display complex and unpredictable behavior. When dealing with confined enclosures, two canonical configurations are typically considered: Rayleigh–Bénard convection, where heating occurs from below and cooling from above, and the differentially heated cavity, where lateral walls are maintained at different temperatures. In the latter case, the imposed temperature gradient induces a circulation loop: fluid rises along the hot wall, moves across the top, descends along the cold wall, and closes the loop along the bottom wall. As the temperature difference between the hot and cold walls increases, the intensity of convection grows, potentially leading to a transition from laminar to turbulent regimes.

This paper focuses on turbulent natural convection of liquid metals in a differentially heated cavity. The study addresses key challenges such as identifying the transition between laminar and turbulent regimes, evaluating suitable turbulence models for low-Prandtl-number fluids, and assessing numerical strategies for accurate simulations. Two standalone codes are employed:

the in-house finite element (FE) code FEMuS [1] and the widely used finite volume (FV) solver OpenFOAM [2]. In addition, a coupled approach is introduced, where FE and FV solvers are integrated through the open-source library MEDCoupling [3], which enables volumetric data exchange.

The paper is organized as follows. First, a review of the available literature and reference benchmarks is presented, with particular attention to the differences between conventional fluids (e.g., water, air) and low-Prandtl-number fluids such as liquid metals. This is followed by an overview of the coupling procedure and algorithm. The results obtained with the standalone FE and FV solvers are then discussed and compared with those of the coupled approach. Finally, the numerical results are validated against benchmark DNS data, emphasizing the capabilities and limitations of each method.

2 BUOYANT DRIVEN DIFFERENTIALLY HEATED CAVITY

The natural convection regime is determined by the Grashof number, $Gr = Ra/Pr$, which is the buoyancy ratio to viscous forces acting on a fluid. The Rayleigh number, Ra, is the dimensionless number that defines the ratio between diffusive and convective thermal transport phenomena, while Pr, the Prandtl number, is defined as the ratio of momentum diffusivity to thermal diffusivity. For a given Pr number, below a critical Ra, conduction dominates heat transfer. As Ra increases, buoyancy strengthens the flow, and the convection term becomes more important. Once Ra exceeds the critical threshold, the flow becomes unsteady, exhibiting periodic motion, and eventually transitions to turbulence. Indeed, it is evident that the critical Rayleigh number itself does not define the transition limit, as the natural convection regime is also closely dependent on the Prandtl number.

According to Lage et al. [4], high-Prandtl number fluids begin the transition to turbulence at a Rayleigh number exceeding 10^8, while low-Prandtl number fluids start the transition at much lower Rayleigh, $Ra \leq 10^5$. As a result, maintaining laminar flow in liquid metal enclosures is challenging, as the flow often becomes turbulent even at relatively low Rayleigh numbers. However, the turbulent regime in this kind of fluid has received limited attention and the available literature data, to the authors' knowledge, is limited to the studies [5, 6, 7, 8, 9, 10].

In [5], Bawazeer et al. conducted a detailed analysis mapping flow regimes in the $Ra - Pr$ domain for steady and unsteady flows, resulting in a correlation relating Pr and the critical Ra number detailed in Equation 1:

$$Ra = 2.8727 \times 10^8 \, Pr^{2.0502} \, . \tag{1}$$

This correlation is illustrated in Figure 1, where the dividing line separates the region of steady solutions, occurring below the critical Rayleigh number, from the region of unsteady solutions above it, where the onset of turbulence emerges. The figure also reports configurations from previous studies. Mohamad et al.[8] investigated transient natural convection while neglecting turbulence terms (circle markers), and later considering them (triangle markers) [9]. Viskanta [7] (plus markers) and Wolf [6] (cross markers) conducted experimental and combined experimental–computational studies, respectively. Finally, Oder et al. [10] (square markers) presented high-fidelity DNS results obtained with a high-order spectral method.

The three $Ra - Pr$ configurations highlighted in red are the considered simulations for this case study. The fluid properties have been adjusted to represent a liquid metal, while variations

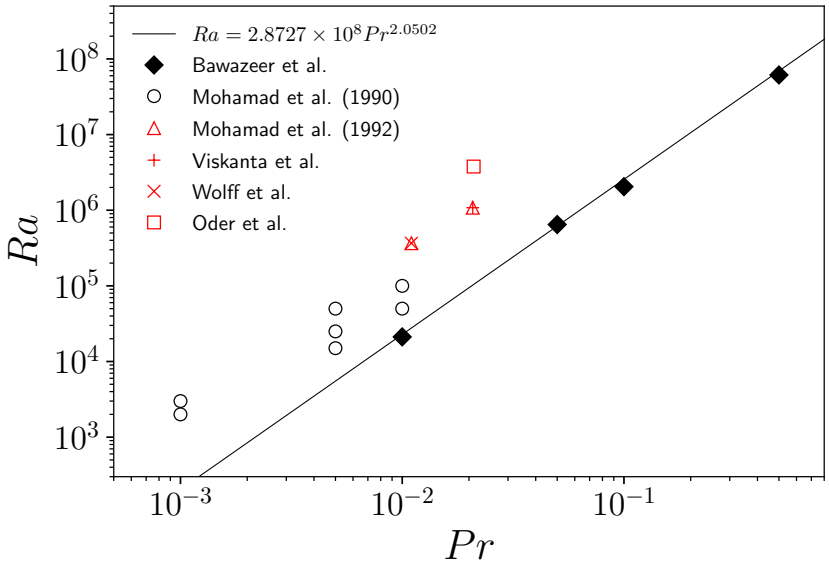

Figure 1: Correlation by Bawazeer et al. from Equation 1 (black line), marking the transition from steady (below) to unsteady (above) flow regimes in low-Prandtl fluids. Black diamond markers refer to the simulations cases conducted in [5]. Circle markers denote critical values predicted by Mohamad et al. [8], triangles point out cases studied by Mohamad et al. [9], and crosses show configurations analyzed by Wolff et al.[6]. DNS case from [10] is indicated using square markers. Those marker coloured in red represent the simulated case configuration in this paper.

in the Rayleigh number have been achieved by modifying the geometry dimensions, keeping the non-dimensional temperature difference between the side walls fixed at 1, and a constant aspect ratio for the cavity ($H/L = 1$). The specifications of the simulated case are depicted in Table 1, where the Grashof number is also reported.

Case	Prandtl	Rayleigh	Grashof	Reference
Simulation 1	0.0210	3.78×10^6	1.8×10^8	[10]
Simulation 2	0.0208	1.08×10^6	5.2×10^7	[7, 11]
Simulation 3	0.0110	3.66×10^5	3.3×10^7	[6, 11]

Table 1: Parameter values (Prandtl, Rayleigh and Grashof numbers) for the simulated cases,

For the sake of conciseness, and because it is the sole case directly comparable with DNS data, only the results of Simulation 1 are presented here. Further details on the other cases can be found in [12].

3 COUPLING ALGORITHM

For the simulation of highly complex problems, it is essential to model multiple physical phenomena arising from different application domains. A representative example is again the simulation of a nuclear reactor, where each physical process is tightly coupled with the others. However, no existing numerical code is capable of handling the full complexity of all physical phenomena simultaneously. Consequently, two main strategies have been developed to address such multiscale and multiphysics problems. The first is the monolithic approach, which consists

of designing a new numerical code capable of modeling all relevant physical processes. The second strategy is the coupling approach, which integrates existing and validated codes in order to enhance simulation capabilities by leveraging their individual strengths. This work follows the latter strategy, focusing on a framework designed for efficient code coupling through direct in-memory data exchange, thereby avoiding input/output operations via external files. Specifically, we present a coupling methodology that exploits the open-source MED and MED-Coupling libraries to link the in-house FEMuS code with the well-established OpenFOAM software. The MED library, developed by the CEA (Commissariat à l'énergie atomique et aux énergies alternatives) and EDF (Électricité de France), is part of the SALOME platform and provides tools for retrieving, processing, and sharing data at the memory level, thus eliminating the need for intermediate disk files.

3.1 Coupling Procedure through the MED Library

This section provides a detailed description of the coupling approach implemented between the two CFD codes, FEMuS and OpenFOAM, which will be employed for the numerical demonstrations presented in the following sections. The procedure can be readily generalized to other software with minimal modifications, primarily by translating the internal data structures into the MED format. The coupling framework is based on three dedicated classes responsible for data retrieval, storage, management, and communication between the two codes. Two of these classes are tailored to each code and serve as intermediaries with the MED library, transferring data from the internal structures of the codes into objects compatible with the MED format. The third class supervises all operations involving MED data. It provides functionality such as interpolating fields defined on meshes with different discretizations, exchanging mesh and numerical field information, and managing both time synchronization and convergence between the codes, thereby ensuring the consistency of the coupled simulation as the solvers advance concurrently. For clarity, in the following we will refer to the finite-volume (FV) and finite-element (FE) solvers simply as Code 1 and Code 2, respectively, to emphasize the interchangeability of the codes within the coupling algorithm.

The coupling process begins with the initialization and setup of the two codes, achieved by creating ghost meshes in MED format. These meshes correspond to either the entire computational domain or to selected subdomains. A specific function of the MED library is devoted to retrieving mesh connectivity, coordinates, and mapping data, which are essential to link the internal data structures of each code with the MED mesh. Once this setup is completed, the interface class is configured, and the time loop can begin. After the first code completes its computation and obtains a solution, the internal fields are transferred into a corresponding MED array. If interpolation is required, a projection function can then be applied. In the present case, for example, FEMuS employs biquadratic fields (P2), whereas OpenFOAM represents data using cell-wise linear fields (P0). Therefore, an alignment of field orders is necessary, which is achieved by converting the FEMuS fields before storing them in the MED ghost mesh. The converted fields can then be transferred to Code 2 directly in memory. With the solution provided by Code 1, Code 2 proceeds to solve its own set of physical equations. Once the solution is obtained, the resulting fields are interpolated from P0 to P2 and passed back to Code 1. At this stage, one coupling step is completed, and the time loop advances to the next iteration.

4 PHYSICAL MODELLING

In the following section a brief description of the FE and FV codes used for the standalone and coupled simulations is given, together with an overview of the equation solved.

4.1 OpenFOAM solver

This study uses the finite volume solver OpenFOAM (Open Field Operation and Manipulation), version 11, developed and maintained by the OpenFOAM Foundation. OpenFOAM is an open-source CFD toolbox widely used for the numerical solution of fluid flow and heat transfer problems, based on the finite volume method and written in C++. It provides a comprehensive set of solvers and libraries for simulating a wide range of engineering-relevant problems, supporting both laminar and turbulent regimes, incompressible and compressible flows, as well as conjugate heat transfer and multiphysics applications, while ensuring full compatibility with parallel computing architectures. Moreover, version 11 introduces modular solvers written as classes, in contrast to the traditional application solvers integral to OpenFOAM in previous versions and different releases. Its open-source nature and active community support make it a reference framework for both academic research and industrial applications.

The governing equations used in the finite element simulations are the RANS equations with the introduction of the Oberbeck-Boussinesq approximation for modeling the buoyancy forces, defined as follows:

$$\frac{\partial \langle u_i \rangle}{\partial x_i} = 0\,, \tag{2}$$

$$\frac{D\langle u_i \rangle}{Dt} = -\frac{1}{\rho}\frac{\partial \langle p \rangle}{\partial x_i} + \frac{\partial}{\partial x_j}\Big[(\nu + \nu_t)\Big(\frac{\partial \langle u_i \rangle}{\partial x_j} + \frac{\partial \langle u_j \rangle}{\partial x_i}\Big)\Big] - g_i \beta \langle T \rangle\,, \tag{3}$$

$$\frac{D\langle T \rangle}{Dt} = \frac{\partial}{\partial x_i}\Big[(\alpha + \alpha_t)\frac{\partial \langle T \rangle}{\partial x_i}\Big]\,. \tag{4}$$

where $\langle u_i \rangle$ is the Reynolds-averaged velocity field, $\langle p \rangle$ the averaged pressure, $\langle T \rangle$ the mean temperature. β is the thermal expansion coefficient, ν the laminar kinematic viscosity, and α the thermal diffusivity, while ν_t and α_t are the turbulent viscosity and turbulent diffusivity, respectively. As can be seen, the Reynolds stress tensor and the turbulent heat flux in OpenFOAM are modeled using the Boussinesq approximation, which assumes a linear relationship between the Reynolds stresses and the mean velocity gradient, and between the turbulent heat flux and the temperature gradient. Depending on the choice of the turbulent model, OpenFOAM models ν_t as a function of the turbulent kinetic energy k and the turbulent dissipation ε, or the specific turbulent dissipation ω. It adopts the Reynolds analogy to determine the turbulent diffusivity as $\alpha_t = \nu_t / Pr_t$ where $Pr_t = 0.85$ is the turbulent Prandtl number, taken as constant by the solver.

The validation of the turbulence model has been performed by comparing four different built-in turbulence models available in OpenFOAM on the same cavity configuration. Without reporting the comparison, the best choice resulted in the standard $k - \omega$ turbulence model by Wilcox [13], which has then been used in the coupled simulation.

4.2 FEMuS solver

The finite element simulations have been carried out using FEMuS, an in-house multigrid C++ library designed for multiphysics applications. The framework builds upon external open-source packages, such as PETSc [14] for managing linear algebra operations and LibMesh [15] for handling the mesh hierarchy. Within FEMuS, several solvers are available, covering incompressible Navier–Stokes flows, heat transfer by convection and conduction, turbulence modeling, fluid–structure interaction, and multiphase phenomena. One of its main design principles is extensibility, which allows for the incorporation of new physical models by formulating the governing constitutive equations directly within the finite element framework. This characteristic allows the library to be adapted to emerging research needs, for example, in the study of turbulent convection in low-Prandtl-number fluids such as liquid metals.

The governing equations used in FEMuS are similar to the considered equations for the FV solver, with a different, more accurate, computation of the Reynolds Stress Tensor $\langle u_i' u_j' \rangle$ and the Turbulent Heat Flux $\langle u_i' T' \rangle$, for which we exploit the Explicit Algebraic Stress Model (EASM) and Explicit Algebraic Heat Flux Model (EAHFM). The equations now hold:

$$\frac{\partial \langle u_i \rangle}{\partial x_i} = 0\,, \tag{5}$$

$$\frac{D\langle u_i \rangle}{Dt} = -\frac{1}{\rho}\frac{\partial \langle p \rangle}{\partial x_i} + \frac{\partial}{\partial x_j}\Big[\nu\Big(\frac{\partial \langle u_i \rangle}{\partial x_j} + \frac{\partial \langle u_j \rangle}{\partial x_i}\Big) - \langle u_i' u_j' \rangle\Big] - g_i \beta \langle T \rangle\,, \tag{6}$$

$$\frac{D\langle T \rangle}{Dt} = \frac{\partial}{\partial x_i}\Big(\alpha \frac{\partial \langle T \rangle}{\partial x_i} - \langle u_i' T' \rangle\Big)\,, \tag{7}$$

$$\langle u_i' u_j' \rangle = f(\nu_t, \nabla \langle u_i \rangle, f_R, f_\tau, \tau_{mg})\,, \tag{8}$$

$$\langle u_i' T' \rangle = f(\nabla \langle u_i \rangle, \langle u_i' u_j' \rangle, f_{RT}, \tau_m)\,. \tag{9}$$

where f_R, f_{RT} are model function and τ_m, τ_{mg} are characteristic thermal and mixed thermal-velocity time scales. The interested reader can find details on the implementation in [16]. Regarding the resolution of the turbulence in the flow, a logarithmic four-parameter $K-\Omega-K_\theta-\Omega_\theta$ turbulence model has been employed, allowing for the solution of the dynamic turbulence and two additional transport equations for the thermal turbulent variable, as stated in [17]. Here, K_θ represents the logarithmic temperature variance and Ω_θ its specific dissipation. The use of logarithmic variables improves the stability of the standard models by ensuring that the state variables remain positive throughout the solution process.

4.3 Coupled equations

The allocation of physical models to each code was determined to best exploit their respective strengths. OpenFOAM was employed to solve the incompressible Navier–Stokes equations (Equations 2, 3), together with the Wilcox k–ω model for the computation of the turbulent dynamic variables. FEMuS, on the other hand, was used to solve the energy equation and to evaluate the turbulent heat flux. The field transfer between the solvers is therefore bidirectional. The FV solver provides velocity and turbulent variables to the FE solver, which in turn uses these fields within the turbulent thermal model to compute the turbulent heat flux, as expressed in Equation 9. This quantity is then employed in the temperature evaluation (Equation 7). The resulting temperature field is subsequently transferred back to OpenFOAM, where it contributes

to the buoyancy term in the momentum equations. This coupling mechanism is illustrated in Figure 2.

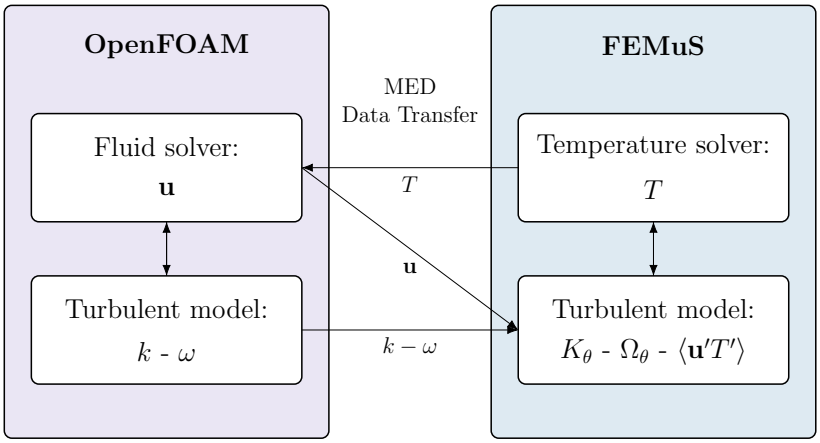

Figure 2: Schematic representation of the coupling strategy between the two solvers.

5 NUMERICAL RESULTS

The test case selected for assessing the volume coupling strategy is the classical differentially heated square cavity ($L = H = 1$), illustrated in Figure 3. The system is modeled as a two-dimensional enclosure filled with an incompressible Newtonian fluid. Heating is applied along one vertical wall (Γ_H), while the opposite wall (Γ_C) is maintained at a lower temperature, thus establishing a temperature gradient across the cavity. The top and bottom boundaries (Γ_w) are assumed adiabatic. Under these conditions, buoyancy forces induced by the thermal gradient drive the flow inside the cavity.

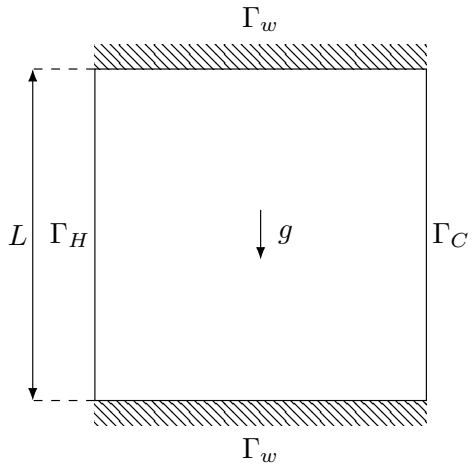

Figure 3: Differentially heated cavity configuration.

In the following, the simulation results are reported in non-dimensional form. Introducing the characteristic velocity scale $u_0 = \sqrt{\beta g \Delta T L}$ the dimensionless velocity is defined

as $U^+ = \sqrt{u^2 + v^2}/u_0$ and the turbulent kinetic energy as $k^+ = k/(u_0^2/2)$. With ΔT denoting the temperature difference between the hot and cold walls, the non-dimensional temperature is expressed as $\Theta^+ = (T - T_{cold})/\Delta T$ and the normalized turbulent heat flux as $\langle u_i' T' \rangle^+ = \langle u_i' T' \rangle / (u_0 \Delta T)$. In this framework, the hot wall corresponds to $\Theta^+ = 1$, while the cold wall corresponds to $\Theta^+ = 0$.

5.1 Coupled Simulations Results

In the following, the results obtained with the Coupled $k-\omega$ approach are compared with the DNS data from Oder et al., and with the solutions of the monolithic solver. The variable profiles are plotted against the non-dimensional x-direction at two different cavity heights: $y+ = 0.5$ (left) and $y^+ = 0.75$ (right).

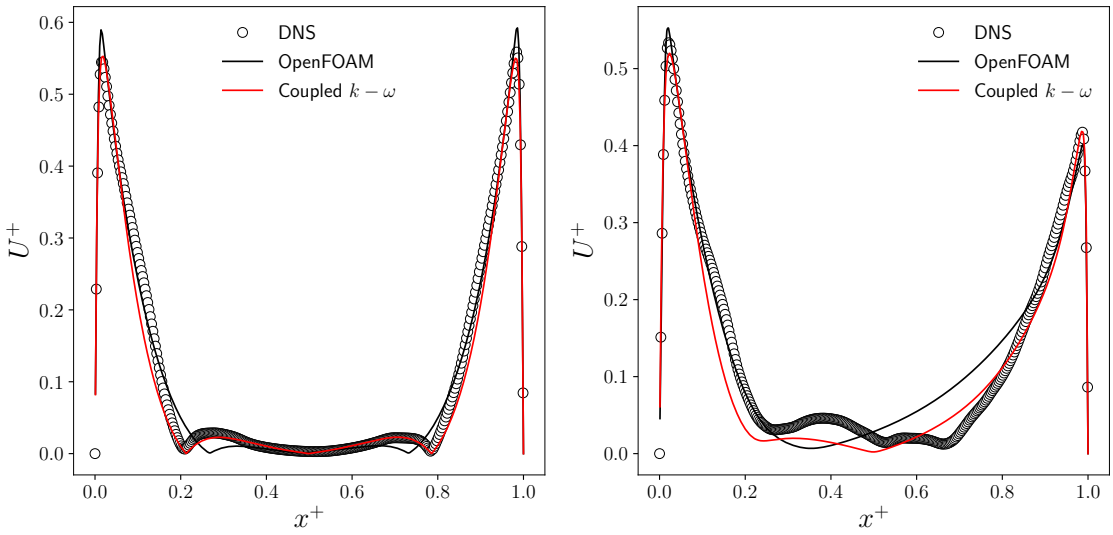

Figure 4: Comparison between DNS (circle marker), coupling application (red line) and monolithic simulations (black line) of the non-dimensional velocity magnitude U^+ for the two heights $y+ = 0.5$ on the left, $y+ = 0.75$ on the right.

Figure 4 illustrates the dimensionless velocity profile. Both monolithic and coupled solutions produce results that are overall consistent with the DNS profile. In particular, the coupled application improves the prediction of velocity peaks and profiles at the center of the cavity, whereas the standalone OpenFOAM simulation shows larger deviations from the DNS profile. Figure 5 reports the dimensionless turbulent kinetic energy. While both approaches correctly capture the location of the peak, they underestimate its magnitude as well as the values in the central region of the cavity. The coupled solution, being based on the FV model, remains close to the OpenFOAM prediction, although the slightly higher peak value represents a promising improvement.

Regarding the thermal fields, Figures 6 and 7 present the non-dimensional temperature distribution and the turbulent heat flux components, respectively. The coupled approach reproduces the temperature profile more accurately than the standalone FEMuS solution, likely as a consequence of the improved velocity field prediction, although the uncoupled simulation still achieves satisfactory agreement. The turbulent heat flux profiles are generally comparable

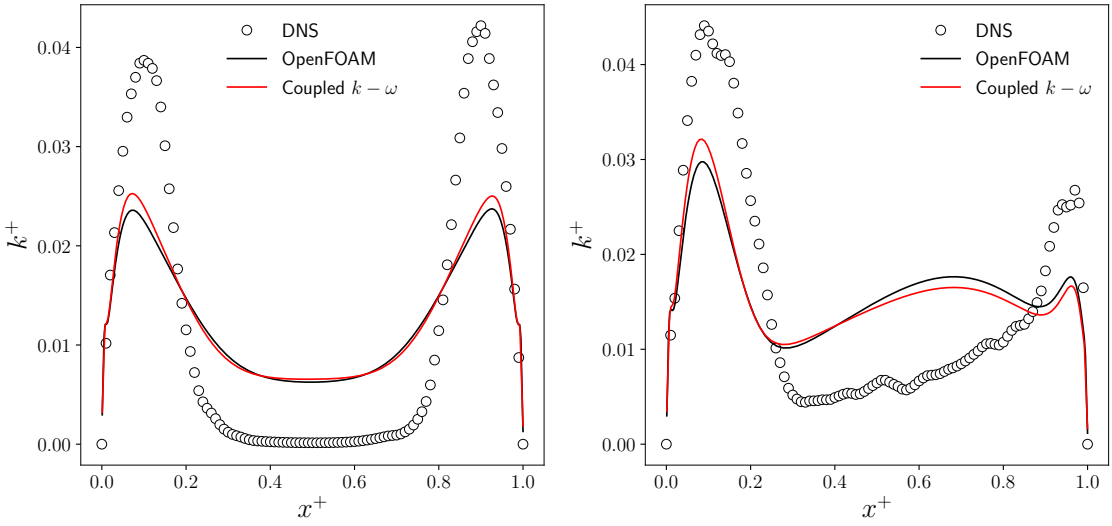

Figure 5: Comparison between DNS (circle marker), coupling application (red line) and monolithic simulations (black line) of the non-dimensional turbulent kinetic energy magnitude k^+ for the two heights $y+ = 0.5$ on the left, $y+ = 0.75$ on the right.

between the two configurations. For the normal component, $\langle u'T' \rangle$, the coupled method underestimates the maximum value, while FEMuS alone slightly overestimates the minimum. For $\langle v'T' \rangle$, the coupled approach smooths the profile by reducing peak magnitudes and simultaneously provides a better match for the minimum values.

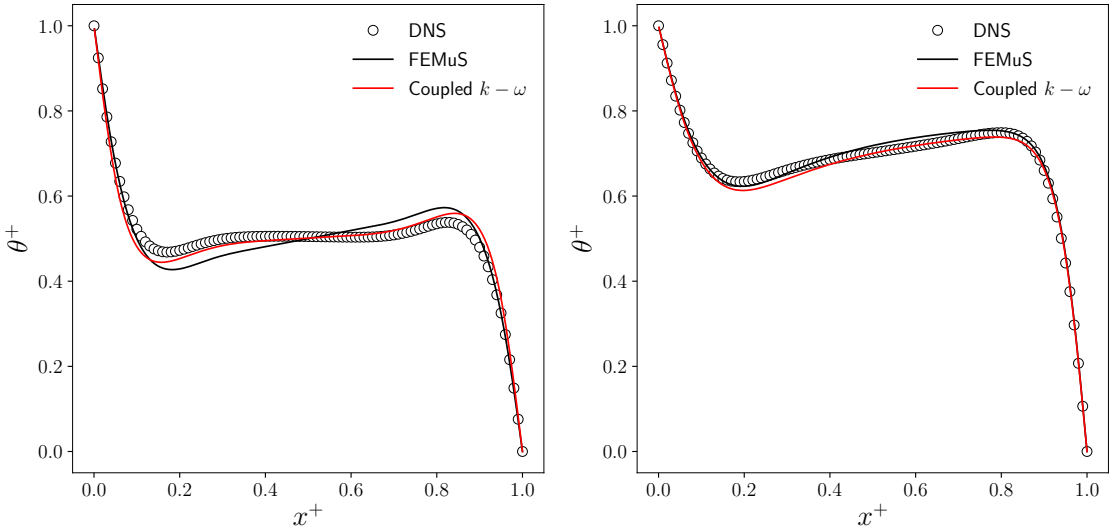

Figure 6: Comparison between DNS (circle marker), coupling application (red line) and monolithic simulations (black line) of the non-dimensional temperature magnitude T^+ for the two heights $y+ = 0.5$ on the left, $y+ = 0.75$ on the right.

Finally, some considerations can be made on the performance of the coupling method in terms of execution time and convergence rate. Figure 8 (top) shows the total execution time as a function of domain resolution for each component of the coupled algorithm, with each solver run on a single core (serial configuration). As observed, the coupling procedure introduces only

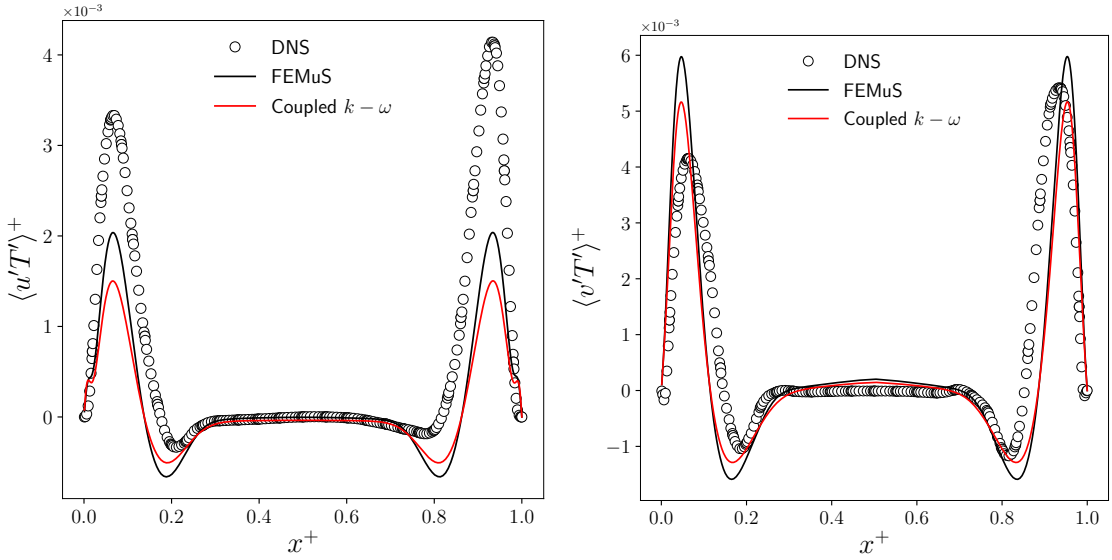

Figure 7: Comparison between DNS (circle marker), coupling application (red line) and monolithic simulations (black line) of the non-dimensional turbulent heat flux components $\langle u'T' \rangle$ (left) and $\langle v'T' \rangle$ (right) for $y+ = 0.5$.

a negligible overhead ($\sim 0.05\%$ of the total time), highlighting its low-intrusive nature. The picture at the bottom instead shows the residual behavior of the two velocity components as a function of the number of iterations to reach the convergence of the solution, compared with the OpenFOAM code in an 80×80 element mesh. The coupling algorithm improves the solution's convergence behavior, achieving the convergence criteria after approximately 6000 iterations, compared to around 7000 iterations required by the standalone OpenFOAM simulation.

6 CONCLUSIONS

This work investigated turbulent natural convection of low-Prandtl-number fluids in a differentially heated cavity using both monolithic solvers and a coupled FE–FV strategy. The coupling framework linked the FEMuS algebraic thermal turbulence model with the dynamic turbulence modeling capabilities of OpenFOAM through volumetric data exchange.

The analysis of velocity profiles shows that both the monolithic and coupled solutions align well with DNS results, with the coupled approach providing a more accurate velocity and temperature prediction of peaks and the central flow region. While the prediction of turbulent kinetic energy and turbulent heat fluxes remains challenging, the coupled results showed encouraging improvements, particularly in the smoothness and alignment of the profiles with reference DNS data. In fact, the coupled approach behaves similarly to OpenFOAM due to its FV-based model, but it slightly improves the peak value. The analysis also highlighted that FEMuS thermal solver performs better when provided with improved dynamic field data, suggesting that employing a more accurate dynamic solver is crucial for simulating such flows. Conversely, OpenFOAM appears less sensitive to improvements in the temperature field, likely due to the simplicity of its turbulence model, which lacks the capability to significantly improve variable predictions based on changes in the thermal field.

Importantly, the coupling procedure introduced negligible computational overhead and even improved convergence rates, confirming its practicality for multiphysics simulations. Overall,

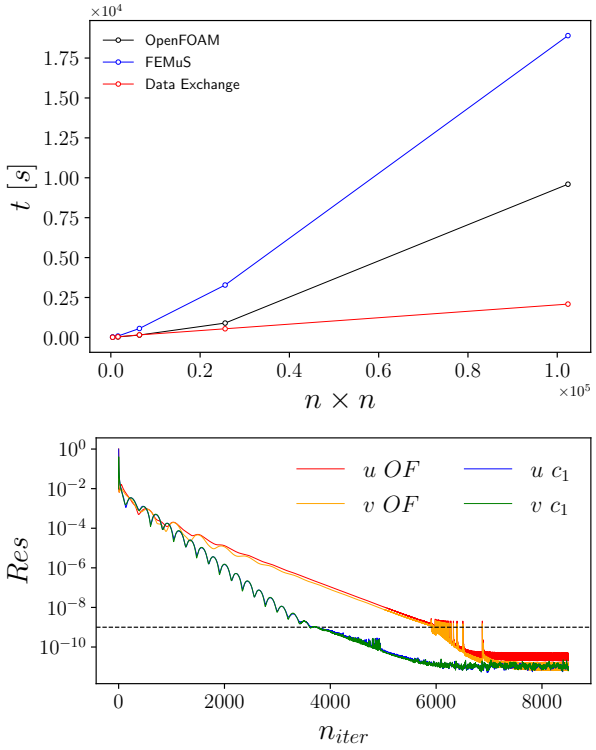

Figure 8: Execution time of the standalone codes, executed in serial, and the coupling procedure plotted against the mesh resolution (top). Residuals of the velocity components as a function of the number of iteration for the FV and the coupled simulation (bottom).

the study demonstrates that coupling heterogeneous solvers can enhance predictive accuracy for complex buoyancy-driven flows in liquid metals. Nevertheless, further investigations are necessary to enhance predictive capabilities, particularly concerning the dynamic behavior of the flow. Future work will focus on extending the methodology to three-dimensional configurations and exploring advanced turbulence closures to further improve predictive capabilities.

REFERENCES

[1] Barbi, G., Bornia, G., Cervone, A., Giovacchini, V., Manservisi S. and others *FEMuS-Platform: A numerical platform for multiscale and multiphysics code coupling*. 9th International Conference on Computational Methods for Coupled Problems in Science and Engineering, COUPLED PROBLEMS 2021 (2021).

[2] Jasak, H., Jemcov, A., and Tukovic, Z. and others, *OpenFOAM: A C++ library for complex physics simulations*. International workshop on coupled methods in numerical dynamics (2007).

[3] Ribes, A., Caremoli, C., *Salome platform component model for numerical simulation*. In Proceedings of the 31st annual international computer software and applications conference, Vol. 2, pp. 553-564 (2007)

[4] Lage, J., and Bejan, A. , *The Ra-Pr domain of laminar natural convection in an enclosure heated from the side*. Numerical heat transfer, Vol. 19, no. 1, pp. 21-41 (1991).

[5] Bawazeer, S., Mohamad, A. and Oclon, P., *Natural convection in a differentially heated enclosure filled with low Prandtl number fluids with modified lattice boltzmann method*. International Journal of Heat and Mass Transfer, Vol. 143, pp. 118562 (2019).

[6] Wolff, F., Beckermann, C. and Viskanta, R., *Natural convection of liquid metals in vertical cavities*. Experimental Thermal and Fluid Science, Vol. 1, no. 1, pp. 83-91 (1988).

[7] Viskanta, R., Kim, D. and Gau, C., *Three-dimensional natural convection heat transfer of a liquid metal in a cavity*. International Journal of Heat and Mass Transfer, Vol. 29, no. 3, pp. 475-485 (1986).

[8] Mohamad, A. and Viskanta, R., *Transient natural convection of low-prandtl-number fluids in a differentially heated cavity*. International Journal for Numerical Methods in Fluids, Vol. 13, no. 1, pp. 61-81 (1991).

[9] Mohamad, A. and Viskanta, R., *Modeling of turbulent buoyant flow and heat transfer in liquid metals*. International Journal of Heat and Mass Transfer, Vol. 36, no. 11, pp. 2815-2826 (1993).

[10] Oder. J., Alsailani, M., Koloszar, L., Munters, W., Laboureur, D., and Pacio, J., *Direct numerical simulation of flow in a confined differentially heated cavity at a low prandtl numbers*. 20th International Topical Meeting on Nuclear Reactor Thermal Hydraulics (NURETH-20). American Nuclear Society, pp. 1206-1218 (2023).

[11] Mohamad, A. and Viskanta, R., *Application of low reynolds number $k-\varepsilon$ turbulence model to buoyant and mixed flows in a shallow cavity*. Fundamentals of Mixed Convection, Vol. 223, pp. 43-54 (1992).

[12] Sirotti, L., *Development of a CFD tool for turbulent natural convection and heat transfer simulations of liquid metals*. PhD thesis, alma (2025).

[13] Wilcox, D. C., *Turbulence modeling for CFD*. DCW Industries, La Canada (1998).

[14] Balay S., Abhyankar S., and others, PETSc Web Page, https://petsc.org/ (2023)

[15] Kirk, S. B., Peterson, J.W., Stogner, R. H., and Carey, G.F., *LibMesh: a C++ Library for Parallel Adaptive Mesh Refinement/Coarsening Simulations*. Engineering with Computers, Vol. 22, no. 3-4, pp. 237-254 (2006)

[16] Barbi, G., Giovacchini, V., and Manservisi, S., *A New Anisotropic Four-Parameter Turbulence Model for Low Prandtl Number Fluids*. Fluids, Vol.7 (2022)

[17] Da Via, R., Giovacchini, V., and Manservisi, S., *A logarithmic turbulent heat transfer model in applications with liquid metals for Pr= 0.01–0.025*. Applied Sciences, Vol. 10, no. 12, p. 4337 (2020)